Contents lists available at SciOpen

Food Science and Human Wellness

journal homepage: https://www.sciopen.com/journal/2097-0765

Metabolite acetyl-*L*-carnitine participates in *Bifidobacterium animalis* F1-7 to ameliorate atherosclerotic inflammation by downregulating theTLR4/NF-κB pathway

Xi Liang[a,b], Zhe Zhang[b], Xiaoying Tian[b], Qingyu Cui[b], Haiyan Lu[b], Maozhen Zhao[b], Tongjie Liu[b], Huaxi Yi[b], Pimin Gong[b,*], Lanwei Zhang[b,*]

[a] *Department of Nutrition and Food Hygiene, School of public health, Qingdao University, Qingdao 266071, China*
[b] *College of Food Science and Engineering, Ocean University of China, Qingdao 266003, China*

ARTICLE INFO

Article history:
Received 21 June 2022
Received in revised form 25 July 2022
Accepted 16 August 2022
Available Online 25 September 2023

Keywords:
Bifidobacterium animalis F1-7
Atherosclerosis
Inflammation
Metabonomics
Acetyl-*L*-carnitine

ABSTRACT

This study aimed to explore the effect of *Bifidobacterium animalis* F1-7 on the improvement of atherosclerotic inflammation. Arteriosclerosis model *ApoE*$^{-/-}$ mice were orally administered with *B. animalis* F1-7 for 12 weeks. The probiotic intervention reduced the plaque areas in aorta and the accumulation of macrophages, and downregulated the expression of toll-like receptor 4 (TLR4)/nuclear factor κB (NF-κB) pathway to reduce the levels of inflammatory factors. The widely-targeted metabolomics analysis showed that acetyl-*L*-carnitine (ALC) in the intestine of atherosclerotic mice was significantly increased after *B. animalis* F1-7 intervention. Correlation analysis proved that ALC was associated with atherosclerotic inflammatory response. By using oxidized low density lipoprotein induced macrophage foam cells, we further verified that ALC could reduce lipid accumulation and inflammatory response in foam cells by downregulating the TLR4/NF-κB pathway. Finally, our results revealed that *B. animalis* F1-7 upregulated the metabolite ALC to downregulate the inflammatory responses, leading to the reduction of plaque accumulation of atherosclerosis.

1. Introduction

Atherosclerosis (AS) related cardiovascular disease is a major public health problem, that has a high mortality rate. The theory of lipid infiltration and inflammation is dominant among the theories of AS pathogenesis[1]. The formation of foam cells by disordered lipid metabolism is closely related to the regulation of cholesterol. Meanwhile, the inflammatory reaction is another key factor to the occurrence of AS[2]. As a key signal transduction receptor of the immune response, toll-like receptor 4 (TLR4) participates in the regulation of the inflammatory response, thus affecting the occurrence and development of AS[3-4]. TLR4 induces the activation of transcription factor nuclear factor-κB (NF-κB), leading to the production of a wide range of pro-inflammatory factors such as tumor necrosis factor-α (TNF-α) and interleukin-1β (IL-1β)[5]. Inhibition of TLR4/NF-κB signaling pathway is a biological target for reducing inflammatory response and anti-atherosclerosis[6].

Studies have found that the diversity of intestinal flora is negatively correlated with the occurrence and development of AS. The lower the amount of variation and the number of microbial species in the gut, the higher the risk of AS. Intestinal microbial metabolites promote the secretion of cytokines by host immune cells and indirectly influence AS by regulating lipid metabolism and inflammation[7]. The widely-targeted metabolomics has been widely used to determine changes in intestinal metabolites. The main purpose is to select metabolites with significant biological and statistical differences among biological samples and on this basis to elucidate the metabolic processes and the mechanisms underlying the observed changes[8-9].

* Corresponding authors at: College of Food Science and Engineering, Ocean University of China, Qingdao 266003, China.
E-mail address: zhanglwanwei@ouc.edu.cn (L.W. Zhang); gongpimin@outlook.com (P.M. Gong)
Peer review under responsibility of Tsinghua University Press.

SciOpen Publishing services by Tsinghua University Press

http://doi.org/10.26599/FSHW.2022.9250069

Probiotics play an important role in balancing and regulating intestinal microbiota diversity and intestinal microbiota metabolites, and participate in various pathways related to intestinal microbiota[10]. Metabolites produced by probiotics can also alter the abundance of other flora and improve AS[11]. *Lactobacillus plantarum* ZDY04 and *Bifidobacterium lactis* Probio-M8 involve in reducing TMAO and improving atherosclerotic cardiovascular disease via the modulation of the gut-heart axes[12-13]. *Lactobacillus fermentum* ZJUIDS06 participates in SCFA to improve lipid metabolism through gut microbiota[14]. The *Bifidobacterium animalis* subsp. *lactis* F1-7 (*B. animalis* F1-7) used in this experiment was isolated from healthy infant feces in our laboratory. In different models, it has been found that *B. animalis* F1-7 effectively reduces lipid metabolism and inflammation, which has the potential to improve atherosclerosis. Therefore, we established the animal model of AS by giving high fat diet to *ApoE*$^{-/-}$ mice. Based on the TLR4/NF-κB pathway, combined with the results of widely-targeted metabolomics, we evaluated the effects of *B. animalis* F1-7 and its metabolites on the inflammatory response of atherosclerotic mice, to identify the specific targets and mechanisms of probiotics in alleviating the AS-related inflammatory response.

2 Materials and methods

2.1 Strain and culture

B. animalis F1-7 was stored in Functional Dairy and Probiotic Engineering Laboratory of the Ocean University of China (No. CCTCC M2020833). The strain was activated for two generations and inoculated in MRS medium at 37 °C for 24 h. The strain was centrifuged at 5 000 × *g* at 4 °C for 5 min. The precipitates were washed twice with phosphate buffered saline and then redissolved with PBS. The viable bacteria amount was adjusted at 1 × 10^8 CFU/mL by colony counting method.

2.2 Mice and experimental design

Ten male C57BL/6J mice and 30 male *ApoE*$^{-/-}$ mice on a C57BL background at 8 weeks of age, weighing 18–20 g, were purchased from Beijing Vital River Laboratory Animal Technology Co., Ltd. (Beijing, China). The animal room was maintained at a constant temperature (21–23 °C) and humidity (40%–60%), with a 12 h light/dark cycle. The mice were fed with normal diet or high fat diet provided by Keao Xieli (Beijing, China). The composition of normal and high fat diets was shown in Table 1. All experiments were approved by the Laboratory Animal Ethics Committee of Ocean University of China (approval number: SPXY2020060502).

After adaptive feeding for 7 days, C57BL/6J mice as the control group were fed with normal diet during the experiment (Control, n = 10). The *ApoE*$^{-/-}$ male mice were fed with high fat diet for 6 weeks, then randomly divided into 3 groups in each group as follows: 1) Atherosclerosis group (AS, n = 10); 2) Drug group (M, n = 10), gavaged with 0.25 mL atorvastatin (10 mg/kg); 3) *B. animalis* F1-7 intervention group (F1-7, n = 10), gavaged with 0.25 mL 1 × 10^8 CFU/mL *B. animalis* F1-7. Both control and AS groups were gavaged with 0.25 mL PBS and the mice in all the groups were given daily gavage. The dose of the drug and probiotic used in this study were similar to those used in previous reports[15-17]. Before the end of the intervention, the feces of the mice were collected and stored at –80 °C for future use.

Table 1
Composition of normal and high fat diets.

Nutrient	Normal diet	High fat diet
Carbohydrates (g/100 g)	52	20
Proteins (g/100 g)	20.1	28
Lipids (g/100 g)	5.9	33
Casein (g/kg)	200	200
L-Cystine (g/kg)	3	3
Corn starch (g/kg)	397	72.8
Maltodextrin (g/kg)	132	100
Sucrose (g/kg)	100	172.8
Cellulose (g/kg)	50	50
Soybean oil (g/kg)	70	25
t-Butylhydroquinone (g/kg)	0.014	25
Lard oil (g/kg)	0	177.50
Mineral mix (g/kg)	35	10
Vitamin mix (g/kg)	10	10
Choline bitartrate (g/kg)	2.5	2
Potassium bitartrate (g/kg)	0	16.50
Calcium carbonate (g/kg)	0	5.5
FD&C Red dye (g/kg)	0	0.05
Dicalcium phosphate (g/kg)	0	13

All mice were sacrificed after 12 weeks of treatment, the mice fasted overnight. After the mice were anesthetized, collected the plasma and centrifuged at 4 000 × *g* for 15 min. The serum was collected and stored at –80 °C. The intestinal tissues and cecal contents were collected and part of the intestinal tissues were fixed with 4% paraformaldehyde fixative, the other part was preserved for other determination. The aortas, aortic roots and arches were excised for histological examination.

2.3 Atherosclerotic lesion analysis

The aortas of the mice were harvested and fixed in 4% paraformaldehyde. 4-μm-thick paraffin-embedded sections of aortas were stained with Oil Red O and H&E staining[18]. The quantification of lesion area and size was performed with Image J software.

2.4 Immunohistochemical analysis

Immunohistochemical staining was performed on the thoracic aortas of the mouse to detect F4/80, NF-κB p65, TLR4 and myeloid differentiation factor 88 (MyD88) (Abcam, UK, 1:500) as previously described[19]. The positively stained area was analyzed by Image J software.

2.5 Measurement of inflammatory cytokines

Inflammatory molecules TNF-α and IL-1β in serum of the mice and macrophage induced foam cells were determined by ELISA assays (Jiancheng, Nanjing, China).

2.6 Quantitative RT-PCR analysis

The transcription levels of *TLR4*, *MyD88*, *NF-κB p65*, *TNF-α* and *IL-1β* genes in ileum tissues and the macrophage-induced foam cells

Table 2
RT-PCR amplified primers.

Gene	Forward (5′-3′)	Reverse (5′-3′)
β-actin	ACTGCTCTGGCTCCTAGCAC	CCACCGATCCACACAGAGTA
TLR4	CACAGAAGAGGCAAGGCGACAG	GAATGACCCTGACTGGCACTAACC
MyD88	AGCAGAACCAGGAGTCCGAGAAG	GGGCAGTAGCAGATAAAGGCATCG
NF-κB p65	TCGAGTCTCCATGCAGCTACGG	CGGTGGCGATCATCTGTGTCTG
TNF-α	GGACTAGCCAGGAGGGAGAACAG	GCCAGTGAGTGAAAGGGACAGAAC
IL-1β	TCGCAGCAGCACATCAACAAGAG	AGGTCCACGGGAAAGACACAGG

were determined, and the method was used the same as in previous study[20]. The mRNA expression amplification primer sequences of related genes are shown in Table 2.

2.7 Western blot analysis

The protein from colon tissues in mice and the macrophage induced foam cells was extracted and the protein concentration was determined using the BCA Protein Assay Kit (Beyotime, China). The samples were separated by SDS polyacrylamide gel electrophoresis, and then transferred to the PVDF membrane. The primary antibody was NF-κB p65 (NF-κB p65, 1:1 000 dilution, Abcam, US), phosphorylated p65 NF-κB (NF-κB p-p65, 1:1 000 dilution, Abcam, US). The internal reference was *β*-actin antibody (diluted at 1:1 000, Abcam, US) and the target proteins were detected with HRP-conjugated secondary antibody (1:7 500 dilution, Cell Signaling, US). The bands were measured with ECL chromogenic kit (Beyotime, China) by using the Bio-Spectrum Imaging Detection System (Tanon, China). Image J software was used for grayscale analysis[21].

2.8 Determination of intestinal metabolites by widely-targeted metabolomics

The intestinal contents of the mice were thawed on ice. A 50 mg (± 1 mg) of each sample was homogenized with 500 μL of ice-cold methanol/water (70%, *V*/*V*) with internal standard. The samples were vortexed for 3 min, sonicated for 10 min in an ice water bath, and vortexed again for 1 min. They were then centrifuged with 12 000 r/min at 4 °C for 10 min. The widely-targeted metabolomics was performed at Wuhan Metware Biotechnology Co., Ltd. (Wuhan, China) as previously described[22-23].

2.9 Cell culture and intervention

RAW264.7 cells were purchased from the cell bank of the Chinese Academy of Sciences (Shanghai, China). RAW264.7 macrophages were induced to form foam cells by oxidized low density lipoprotein (ox-LDL). The RAW264.7 cells were grown to 80% with high glucose DMEM medium containing 10% FBS and 1% double antibody in the cell incubator at 37 °C and 5% CO_2. The RAW264.7 cells were planted in a 6-well plate at a density of 5×10^5 cells per well. The intervention of cell experiment was divided into three groups: 1) The control group was added with medium; 2) The ox-LDL group was added with 50 μg/mL ox-LDL (Yiyuan, China); 3) The acetyl-*L*-carnitine (ALC) group was treated with 50 μg/mL of ox-LDL and 10 mmol/L of ALC (Sigma Aldrich, US). These concentrations were based on those used in previous studies[24-25]. After 24 h of intervention, the cells were collected for subsequent experiments.

2.10 Determination of lipid accumulation in macrophage-induced foam cells

The cell medium was discarded and the macrophage induced foam cells were washed twice with PBS, fixed with 4% paraformaldehyde fix solution for 2 h, and stained with Oil Red O and Bodipy[26]. The accumulation of lipid droplets in the cells was observed using an inverted microscope (Olympus, Japan).

2.11 Statistical analysis

All data were analyzed statistically with SPSS v.22.0 software and presented as mean ± standard deviation. One-way analysis of variance and Tukey-Kramer Test were used to analyze the differences among the groups. $P < 0.05$ was considered statistically significant. Each experiment was repeated three times.

3. Results

3.1 B. animalis F1-7 reduced aortic plaque accumulation in mice

The results of H&E and Oil Red O staining of the aortic sinus showed that, compared with the control group, the intimal integrity was damaged in the arterial sections of AS group (Fig. 1A). A large number of foam cells and inflammatory cells accumulated in the intima. The AS group showed significant atherosclerotic plaques formation in the aorta. The plaque area was significantly reduced in the drug group and *B. animalis* F1-7 group than that in the AS group. The red stained lipid area was analyzed, and the percentage of the lipid area to the total area was calculated (Fig. 1B). Compared with AS group, the plaque area was significantly reduced in the M group (decreased by 63.8%) and the *B. animalis* F1-7 group (decreased by 52.8%) ($P < 0.05$). There was no significant difference between the M group and the *B. animalis* F1-7 group ($P > 0.05$).

3.2 B. animalis F1-7 improved the levels of serum inflammatory factors in mice

Changes in serum inflammatory factors were shown in Fig. 2.

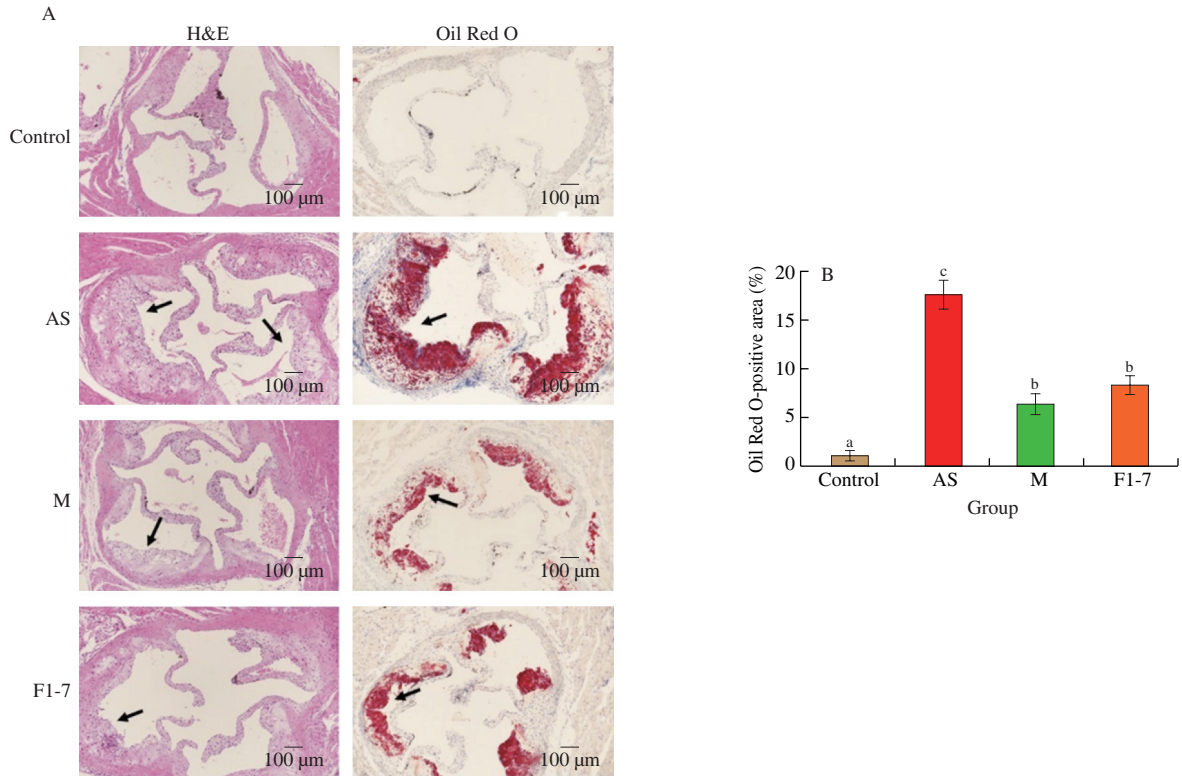

Fig. 1 (A) H&E and Oil Red O staining of transverse sections of the aortic sinus and (B) the plaque lipid content were assessed by Oil Red O staining. Different letters indicated significant differences ($P < 0.05$). The arrow points to the plaques of the aorta.

The serum level of TNF-α in atherosclerotic mice was significantly increased by the high fat diet. Both the M group and the *B. animalis* F1-7 group reduced the TNF-α level ($P < 0.05$). Compared with the control group, the level of IL-1β in serum of *ApoE*$^{-/-}$ mice in AS group was increased by 2 times. *B. animalis* F1-7 effectively reduced the expression of IL-1β, and there was no difference in the effect with the drug ($P > 0.05$).

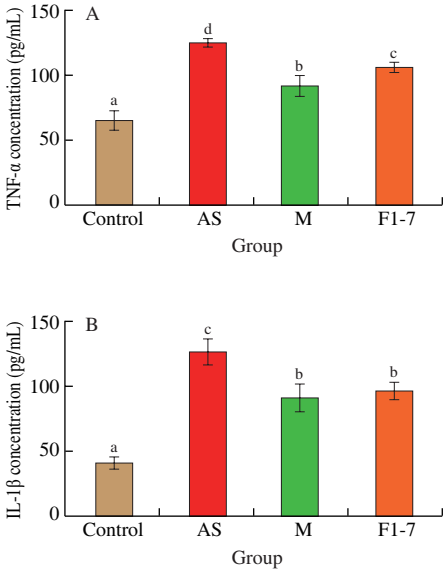

Fig. 2 Effects of *B. animalis* F1-7 administration on serum pro-inflammatory cytokines. Serum (A) TNF-α and (B) IL-1β levels. Different letters indicated significant differences ($P < 0.05$).

3.3 B. animalis F1-7 alleviated inflammation in mice aortic sinus of ApoE$^{-/-}$ *mice*

Immunohistochemical results of F4/80 showed that the positive area in aortic plaques of atherosclerotic mice induced by high fat diet was significantly increased, compared with that of normal mice ($P < 0.05$) (Fig. 3). It was indicated that the content of macrophages was increased in AS group. After treatment with the drug and *B. animalis* F1-7, the F4/80 positive area was significantly reduced ($P < 0.05$). The TLR4 positive area in aorta sinus of atherosclerotic mice was significantly elevated. The expression of TLR4 in the AS group was 2.1 times higher than that in the control group ($P < 0.05$). The *B. animalis* F1-7 group was able to reduce the TLR4 positive area. There was no significant difference with the M group. The high fat diet activated the inflammatory response pathway, leading to aortic inflammation. The expression of MyD88 and NF-κB p65 was upregulated in the AS group. *B. animalis* F1-7 intervention effectively downregulated their expression, reducing the positive areas of MyD88 and NF-κB p65 in aorta and improving the inflammatory response ($P < 0.05$).

3.4 B. animalis F1-7 decreased the gene expression of inflammation in mice intestine

The expression of intestinal inflammation related genes was measured, and the results were shown in Fig. 4A. High fat diet increased the expression of inflammatory factors in the intestine of

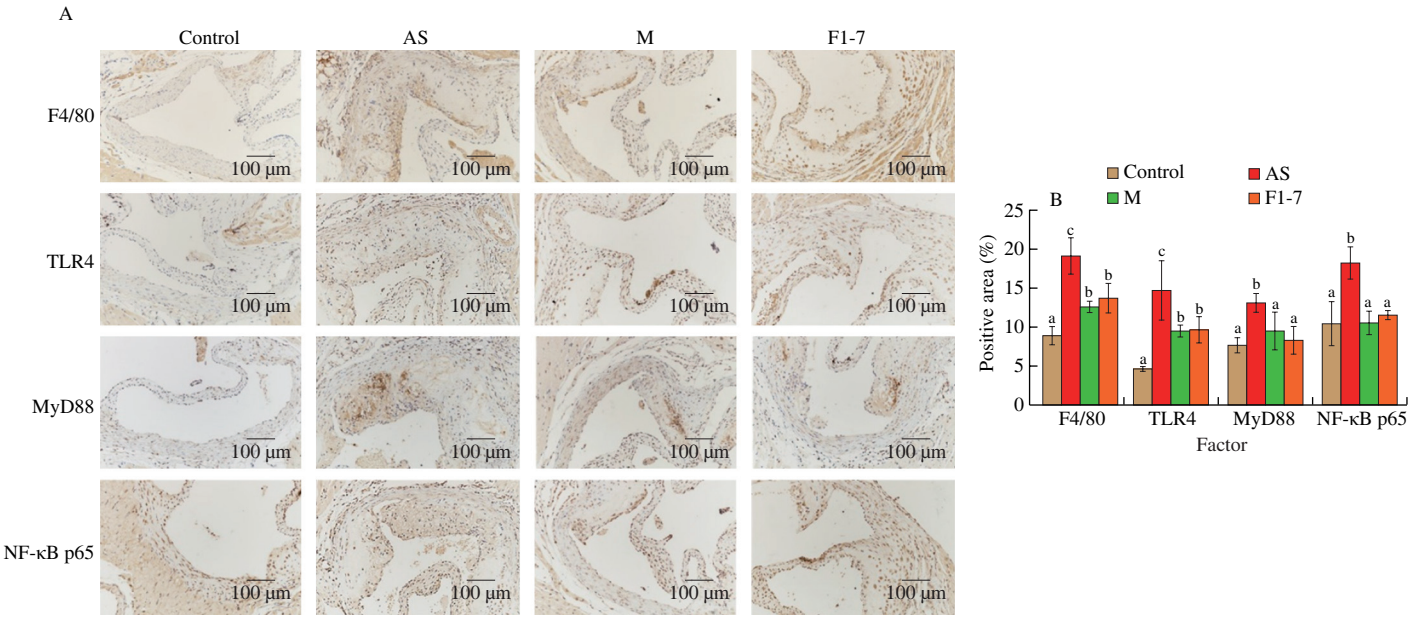

Fig. 3 Effects of *B. animalis* F1-7 on aortic sinus inflammation in atherosclerotic mice. (A) F4/80, TLR4, MyD88, NF-κB p65 expression in atherosclerosis plaque was measured by immunohistochemistry. (B) Quantitative analysis of F4/80, TLR4, MyD88 and NF-κB p65 by Image J software. Different letters indicated significant differences, $P < 0.05$.

ApoE$^{-/-}$ mice. Compared with the AS group, after treatment with the drug and *B. animalis* F1-7, *TNF-α* was significantly downregulated ($P < 0.05$). The *IL-1β* expression in AS group was increased by 2.9 fold compared to the control group, and the *B. animalis* F1-7 downregulated the *IL-1β* expression by 40.5%. Meanwhile, compared with the AS group, *B. animalis* F1-7 effectively downregulated the gene expressions of *TLR4*, *MyD88* and *NF-κB p65* in *ApoE*$^{-/-}$ mice, and there was no statistical difference with the M group. High fat diet increased the protein expression of NF-κB p65 and the phosphorylation level of p65 in the intestinal tract of the *ApoE*$^{-/-}$ mice, and activated the inflammatory pathway. *B. animalis* F1-7 effectively reduced the NF-κB p65 and its phosphorylated protein level (Fig. 4B). Both probiotic and drug effectively improved inflammation, according to the analysis, there was no significant difference between the two groups ($P > 0.05$) (Fig. 4C).

3.5 Changes in mice intestinal metabolites after B. animalis F1-7 intervention by widely-targeted metabolomics analysis

The widely-targeted metabolomics was used to analyze the differences of intestinal metabolites between the AS and *B. animalis* F1-7 groups. Three key parameters R^2_X, R^2_Y and Q^2 were obtained by the Orthogonal partial least squares discriminant analysis (OPLS-DA) analysis, which were 0.606, 0.993 and 0.549, respectively. Permutation testing of the model's quality (Fig. 5A) indicated that the model was not over fitted. OPLS-DA score showed that there were significant differences in the intestinal metabolic profiles between the AS group and the *B. animalis* F1-7 group (Fig. 5B). A total of 48 metabolites (downregulated, 25; upregulated, 23) were significantly different between the AS group and the *B. animalis* F1-7 group. The fold change (FC) values of the metabolites between the two groups were calculated. After the differential multiple $\log_2$ treatment, the top 20 metabolites with the largest changes were displayed in bar chart (Fig. 5C) and the top 10 metabolites with the largest FC values were selected for radar map (Fig. 5D). These were mainly included aliphatic acylates, bile acids and sterol esters. The pathway-associated metabolite sets (SMPDB) was selected for enrichment analysis of differential metabolites. These potential biomarkers were mainly enriched in 25 pathways, such as the beta oxidation of very long chain fatty acids pathway, carnitine synthesis, bile acid biosynthesis and biotin metabolism pathway (Figs. 5E-F). Among the top 10

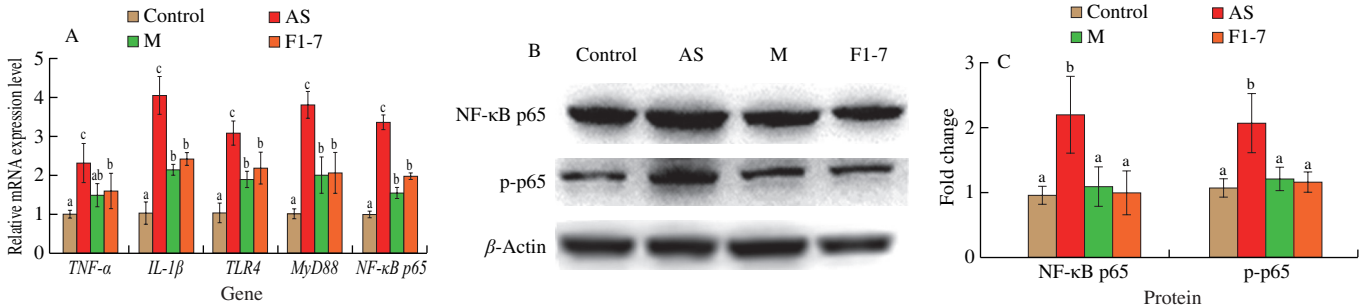

Fig. 4 Effect of *B. animalis* F1-7 on intestinal inflammatory response. (A) Relative changes of *TNF-α*, *IL-1β*, *TLR4*, *MyD88* and *NF-κB p65* gene expression in mouse intestine were measured by real-time PCR. (B) The protein expression of NF-κB p65 and p-p65 were determined by Western blotting. (C) Quantitative data of NF-κB p65 and its phosphorylation in intestine normalized with *β*-actin. Different letters indicated significant differences ($P < 0.05$).

metabolites, ALC (detection index number, MEDP0510), as carnitine derivatives, has been implicated in metabolic pathways, such as fatty acid β-oxidation, energy metabolism and anti-inflammatory. We then conducted a correlation analysis between ALC and key indicators of AS (Fig. 5G). It was found that the ALC was highly correlated with atherosclerotic plaque area, the serum indicators TG and TC, and inflammatory indicators, especially TNF-α. The ALC of the *B. animalis* F1-7 group was significantly increased, 2.5 times higher than that of the AS group (Fig. 5H). According to the results, ALC might be a key metabolite affecting the inflammatory response in AS.

3.6 *Effects of ALC on lipid accumulation and inflammation in foam cells*

To further verify the effect of ALC on atherosclerotic inflammation, the ox-LDL was used to induce RAW264.7 cells to construct a foam cell model *in vitro*. The amount of lipid phagocytosis in the cells significantly increased after the ox-LDL intervention. On this basis, the administration of ALC intervention can effectively reduce the phagocytosis of macrophages with ox-LDL, thus reducing the generation of foam cells. As shown in Fig. 6A, the Oil Red O treated foam cells showed the presence of colored lipid droplets of

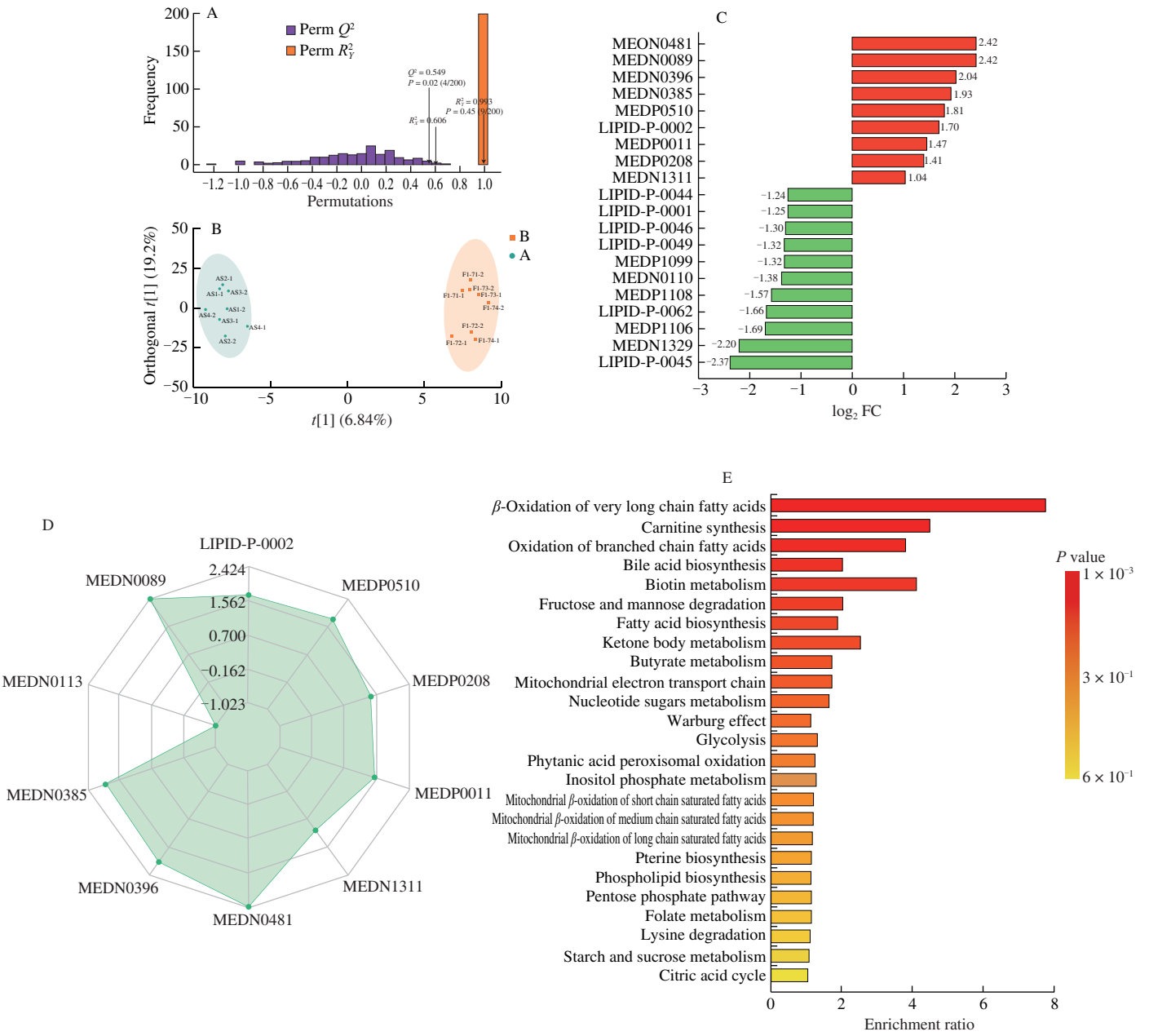

Fig. 5 Effects of *B. animalis* F1-7 on metabolomics of cecal content in *ApoE*$^{-/-}$ mice. (A) The principal component analysis (PCA) model of metabonomic data from AS and *B. animalis* F1-7 groups. (B) OPLS scores plot of the AS and *B. animalis* F1-7 groups. (C) The bar chart of top 20 upregulated metabolites and down-regulated metabolites between AS and *B. animalis* F1-7 groups. (D) Radar plots of the top 10 differential metabolites with maximum FC values. (E) The biomarker enrichment analysis by SMPDB. (F) The biomarker metabolic pathway map. (G) Correlation analysis of differential metabolite ALC and key indicators of atherosclerosis. *$P < 0.05$ and **$P < 0.01$. (H) The Raw intensity of ALC in AS and *B. animalis* F1-7 groups. Different letters indicated significant differences ($P < 0.05$).

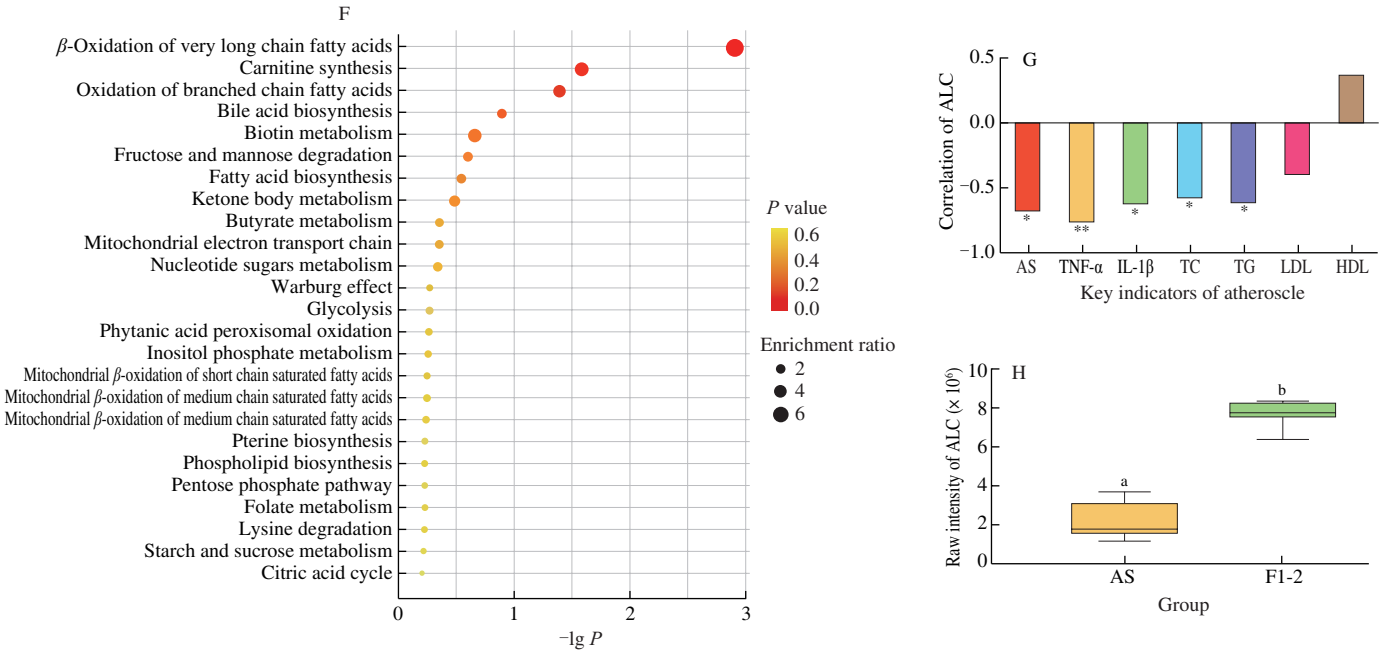

Fig. 5 (*Continued*)

varying sizes around individual cells. After ALC administration, the number of lipid droplets around the cells was significantly reduced. Bodipy staining showed that the fluorescence intensity in the foam cell model group was significantly increased, and ALC significantly reduced the fluorescence intensity (Fig. 6B). These results showed that ALC improved the intracellular lipid accumulation and reduced the formation of foam cells.

3.7 *Effects of ALC on inflammatory cytokines in foam cells*

The inflammatory cytokines in foam cells of each group were determined. Compared with the control group, the TNF-α in ox-LDL group was significantly increased, and the foam cells secreted more pro-inflammatory factors, which increased the inflammatory response. ALC reduced the inflammatory level of foam cells, downregulated TNF-α, as shown in Fig. 7A. Ox-LDL intervention also increased the IL-1β level, which was downregulated by ALC. There was no significant difference between the ALC and control groups (Fig. 7B).

The gene expression related to inflammatory response in each group was measured, as shown in Fig. 7C. The expression of *TLR4* was 2 times higher in ox-LDL group and significantly downregulated in ALC group. The changes of *MyD88* and *NF-κB p65* were consistent with those of *TLR4*, and the expression levels in ox-LDL group were increased by more than 1 time ($P < 0.05$). After the intervention with ALC, the gene expression levels were restored to the levels of the control group. The expression of *TNF-α* in ox-LDL group was upregulated by 2 times compared with the control group. After ALC intervention, the expression of *TNF-α* was downregulated by 48% compared with ox-LDL group. the expression of *IL-1β* was significantly increased in the foam cells. On the basis of this, the

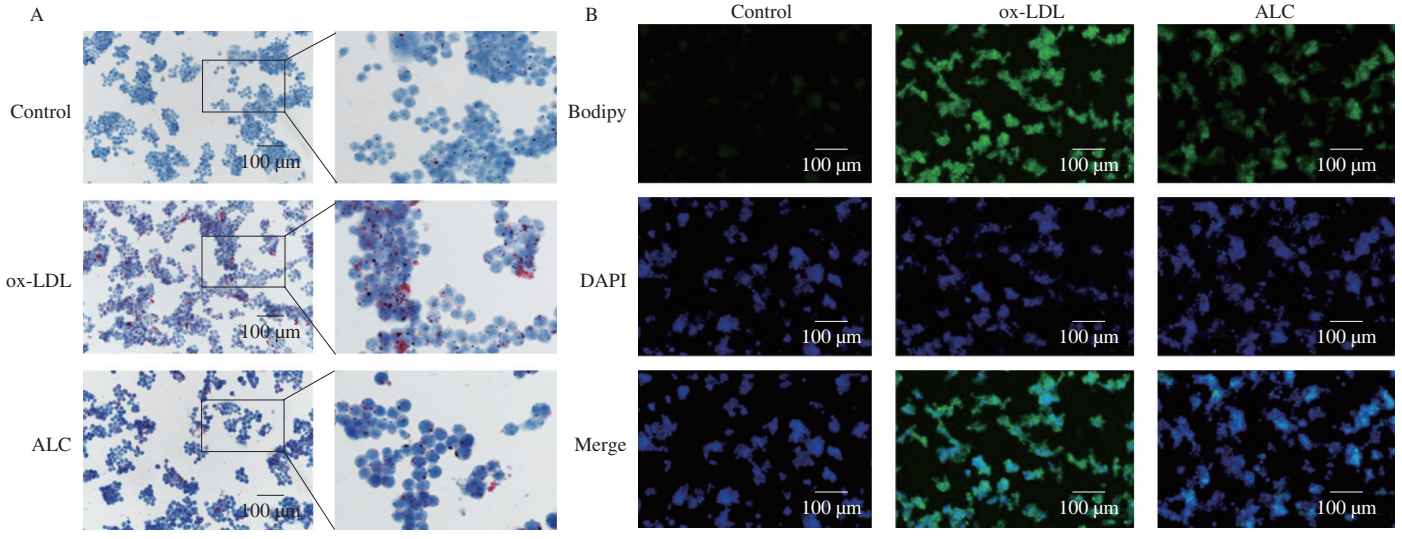

Fig. 6 RAW264.7 cells treated with or without ALC (10 μmol/L) were incubated with or without ox-LDL (50 μg/mL) for 24 h. (A) Oil red O and (B) Bodipy staining was performed.

expression of *IL-1β* was effectively reduced by ALC, which was decreased by 31% compared with ox-LDL group.

From the perspective of protein expression, it was found that the levels of NF-κB p65 and p-p65 in macrophage-foam cells induced by ox-LDL were significantly increased ($P < 0.05$) (Figs. 7D-E). While ALC effectively downregulated the expression of NF-κB p65 and NF-κB p-p65 to the normal levels. In summary, the results indicated that ALC had the ability to reduce the expression of pro-inflammatory factors and improve inflammatory response by downregulating the TLR4/NF-κB pathway.

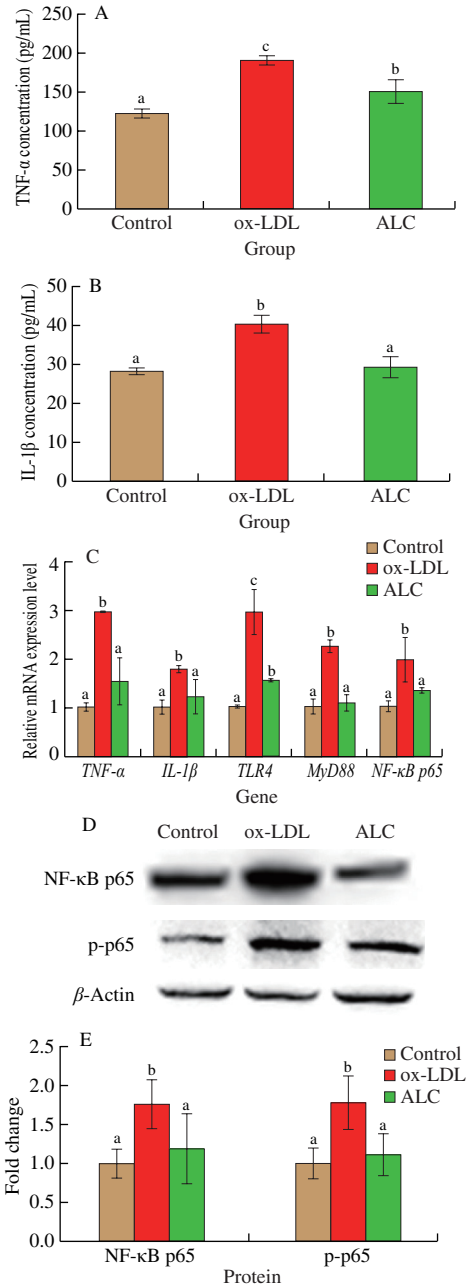

Fig. 7 Effects of ALC administration on proinflammatory cytokine (A) TNF-α and (B) IL-1β levels in foam cells. (C) Relative mRNA expression levels of the inflammatory factors in foam cells, contain the genes of *TNF-α*, *IL-1β*, *TLR4*, *MyD88* and *NF-κB p65* by quantitative reverse-transcription PCR analyses with *β-actin* as the internal reference. (D) The protein expression of NF-κB p65 and p-p65 were determined by Western blotting. (E) Quantitative data of NF-κB p65 and its phosphorylation in foam cells normalized with *β*-actin. Different letters indicated significant differences ($P < 0.05$).

4. Discussion

The development of atherosclerotic plaques involves abnormal inflammatory cell recruitment and foam cell formation[27-28]. Inflammation plays a key role in the occurrence and development of AS[29]. Probiotics can alter the intestinal flora and its metabolites to improve atherosclerotic cardiovascular diseases, but the mechanism remains unclear. Therefore, this study evaluated the changes of biochemical indexes and inflammatory response related gene expression in AS model mice from the perspective of inflammation. Combined with the results of widely-targeted metabolomics, clarified the specific mechanism of *B. animalis* F1-7 in improving AS.

Studies have shown that many immune inflammatory cells and cytokines are involved in the occurrence and development of the inflammatory response, among which macrophages are the main components of atherosclerotic plaques. Activated macrophages are involved in advanced AS lesions together with other immune cells. Monocytes differentiate into M1 and M2 macrophages using monocyte colony stimulating factors[30]. Ox-LDL uptake by M1 macrophages plays an important role in the formation of foam cells and in the rupture of atherosclerotic plaques[31]. Our study found that administration of *B. animalis* F1-7 reduced the accumulation of M1 macrophages in aorta and reduced the aortic plaque formation of the *ApoE*$^{-/-}$ mice. TLR4 is highly expressed in endothelial cells and macrophages in atherosclerotic plaques, and is a transmembrane protein on the cell surface, mainly recognizing microbial membrane components[32]. TLR4 binds to the MyD88 receptor to trigger downstream signaling cascades that lead to phosphorylation of activated serine protein kinase (MAPK) and the NF-κB, leading to transcription and expression of downstream pro-inflammatory cytokines such as TNF-α and IL-1β[33-35]. The transcription factor NF-κB regulates numbers of genes that involve in immune and inflammatory responses[36]. p65 (RELA) is one of the subunits of NF-κB transcription factor family and functions predominately as a transcription activator of pro-inflammatory cytokines[37]. Posttranscriptional modification, such as phosphorylation, of p65 upon stimulation dictates the canonical mechanism for its nuclear translocation and activation[38]. We found that *B. animalis* F1-7 markedly suppressed NF-κB activation and posttranscriptional modification. In support of this observation, Li et al.[39] reported that *B. animalis* reduced phosphorylated NF-κB p65 activation in HT-29 cells. A previous study by Yang et al.[40] have shown that lactate suppresses NF-κB activation and nuclear translocation in RAW264.7 cells. In agreement, we observed that *B. animalis* F1-7 decreased phosphorylation of p65 was accompanied by suppressed expression of TNF-α and IL-1β levels in *ApoE*$^{-/-}$ mice and macrophage-induced foam cells. These results suggest that *B. animalis* F1-7 may exert a potent anti-inflammatory in intestinal tract and aortic plaques through downregulating TLR4/NF-κB pathway.

Changes in the intestinal microbiota are directly related to cardiovascular diseases, intestinal microbiota metabolites influence the formation of atherosclerotic plaques by influencing a variety of metabolic pathways[41]. According to the results of the widely-targeted metabolomics, we found that the intestinal metabolites of mice were significantly changed after they were given a high fat diet. The probiotic intervention effectively altered the composition of intestinal metabolites. By analyzing the differential metabolites between the

model group and the *B. animalis* F1-7 group, we identified the specific differential metabolite ALC. Enrichment analysis of differential metabolites by SMPDB also suggested that some differential metabolites caused significant changes in the Carnitine Synthesis pathway. ALC is the prominent acetylated derivative of carnitine. This compound is synthesized by carnitine acetyl-transferase which catalyzes the acetylation of carnitine[42]. In mammalian carnitine pools, ALC is the most significant quantitatively and functionally, with better bioavailability and antioxidant capacity[43]. ALC is one of metabolites within the TMAO-choline/carnitine gut microbiota pathway and a key component of long-chain fatty acids transportation process through mitochondrial membrane into the matrix where they go through β-oxidation[44]. The intestinal metabolite ALC in *ApoE*$^{-/-}$ mice was significantly increased after *B. animalis* F1-7 intervention. Studies had reported that ALC could improve inflammatory response and oxidative stress through TLR4/NF-κB pathway[45]. It could also reduce atherosclerotic plaque accumulation by acting on CRP and TNF-α[46]. Through correlation analysis, we found that ALC was highly negatively correlated with atherosclerotic plaque area, serum lipids, especially inflammatory indicators. It was speculated that ALC might be a potential functional component affecting the inflammatory response of AS. Therefore, ox-LDL-induced macrophage foam cell model was constructed to verify the effects of ALC on AS-associated inflammation *in vitro*.

TLR4 expression was significantly increased in ox-LDL induced foam cells in a dose- and time-dependent manner[47]. Similarly, our study found that ox-LDL intervention in macrophages significantly increased the expression of TLR4. On this basis, the administration of ALC effectively downregulated TLR4 and related inflammatory targets, reduced the generation of foam cells. The intestinal flora could metabolize *L*-carnitine, which could be converted to ALC and perform its biological function[48]. Therefore, it was speculated that *B. animalis* F1-7 might be directly involved in the acetylation process of carnitine or act on intestinal flora to affect the content of metabolite ALC, regulating the TLR4/NF-κB pathway and ultimately improving atherosclerotic inflammation. The specific mechanism still requires further exploration.

5. Conclusion

B. animalis F1-7 could improve AS by regulating the inflammatory response in *ApoE*$^{-/-}$ mice. The widely-targeted metabolomics analysis showed that ALC, in the intestinal tract of atherosclerotic mice, was significantly increased after probiotic intervention and was closely related to the inflammatory response. The mechanism might be that the probiotic regulated the expression of key genes in TLR4/NF-κB pathway by increasing the content of ALC in the intestine, improving the inflammatory response, and ultimately reducing the plaque accumulation of AS. At the same time, the foam cell model was constructed to verify that ALC could reduce the lipid accumulation and inflammatory response through TLR4/NF-κB pathway. However, the source of intestinal ALC and related intestinal microbiota analysis still need to be further explored. Furthermore, combined with the previous study on the lipid-lowering ability of the strain, *B. animalis* F1-7 could regulate AS through multiple pathways, which has promising commercial and scientific implications.

Conflicts of interest

The authors declare that they have no known competing financial interests or personal relationships that could have appeared to influence the work reported in this paper.

Acknowledge

This work was supported by Shandong Taishan industry leading talent project (LJNY202101), and the National Key R & D of China (2018YFC0311201).

Ethical approval

This study was conducted according to the guidelines of the Animal Care and were approved by the Laboratory Animal Ethics Committee of Ocean University of China (approval number: SPXY2020060502).

References

[1] N. Wang, X. Zhang, Z. Ma, et al., Combination of tanshinone IIA and astragaloside IV attenuate atherosclerotic plaque vulnerability in *ApoE*$^{-/-}$ mice by activating PI3K/AKT signaling and suppressing TRL4/NF-κB signaling, Biomed. Pharmacother. 123 (2020) 109729. https://doi.org/10.1016/j.biopha.2019.109729.

[2] M. Bäck, A. Yurdagul, I. Tabas, et al., Inflammation and its resolution in atherosclerosis: mediators and therapeutic opportunities, Nat. Rev. Cardiol. 16 (2019) 389-406. https://doi.org/10.1038/s41569-019-0169-2.

[3] Z. Ye, L. Zhong, S. Zhu, et al., The P-selectin and PSGL-1 axis accelerates atherosclerosis via activation of dendritic cells by the TLR4 signaling pathway, Cell Death Dis. 7 (2019) 507. https://doi.org/10.1038/s41419-019-1736-5.

[4] A. Piaszyk-Borychowska, L. Széles, A. Csermely, et al., Signal integration of IFN-I and IFN-II with TLR4 involves sequential recruitment of STAT1-complexes and NFκB to enhance pro-inflammatory transcription, Front. Immunol. 10 (2019) 1253. https://doi.org/10.3389/fimmu.2019.01253.

[5] X. Zhang, C. Xue, Q. Xu, et al., Caprylic acid suppresses inflammation via TLR4/NF-κB signaling and improves atherosclerosis in ApoE-deficient mice, Nutr Metab (Lond). 16 (2019) 40. https://doi.org/10.1186/s12986-019-0359-2.

[6] J.D. Bowman, S. Surani, M.A. Horseman, et al., Toll-like receptor-4, and atherosclerotic heart disease, Curr. Cardiol. Rev. 13 (2017) 86-93. https://doi.org/10.1186/s12986-019-0359-2.

[7] L.J. Kasselman, N.A. Vernice, J. DeLeon, et al., The gut microbiome and elevated cardiovascular risk in obesity and autoimmunity, Atherosclerosis 271 (2018) 203-213. https://doi.org/10.1016/j.atherosclerosis.2018.02.036.

[8] Y. Xiao, X. Li, X. Zeng, et al., A low *ω*-6/*ω*-3 ratio high-fat diet improves rat metabolism via purine and tryptophan metabolism in the intestinal tract, while reversed by inulin, J. Agric. Food Chem. 67 (2019) 7315-7324. https://doi.org/10.1021/acs.jafc.9b02110.

[9] X. Jian, Y. Zhu, J. Ouyang, et al., Alterations of gut microbiome accelerate multiple myeloma progression by increasing the relative abundances of nitrogen-recycling bacteria, Microbiome 8 (2020) 74. https://doi.org/10.1186/s40168-020-00854-5.

[10] W.H.W. Tang, D.Y. Li, S.L. Hazen, Dietary metabolism, the gut microbiome, and heart failure, Nat. Rev. Cardiol. 16 (2019) 137-154. https://doi.org/10.1038/s41569-018-0108-7.

[11] L.E. London, A.H. Kumar, R. Wall, et al., Exopolysaccharide-producing probiotic *Lactobacilli* reduce serum cholesterol and modify enteric microbiota in ApoE-deficient mice, J. Nutr. 144 (2014) 1956-1962. https://doi.org/10.3945/jn.114.191627.

[12] B. Sun, T. Ma, Y. Li, et al., *Bifidobacterium lactis* Probio-M8 adjuvant treatment confers added benefits to patients with coronary artery disease via target modulation of the gut-heart/-brain axes, mSystems 7 (2022) e0010022. https://doi.org/10.1128/msystems.00100-22.

[13] L. Qiu, X. Tao, H. Xiong, et al., *Lactobacillus plantarum* ZDY04 exhibits a strain-specific property of lowering TMAO via the modulation of gut microbiota in mice, Food Funct. 9 (2018) 4299-4309. https://doi.org/10.1039/c8fo00349a.

[14] D. Yang, W. Lyu, Z. Hu, et al., Probiotic effects of *Lactobacillus fermentum* ZJUIDS06 and *Lactobacillus plantarum* ZY08 on hypercholesteremic golden hamsters, Front. Nutr. 28 (2021) 705-763. https://doi.org/10.3389/fnut.2021.705763.

[15] S. Peng, L.W. Xu, X.Y. Che, et al., Atorvastatin inhibits inflammatory response, attenuates lipid deposition, and improves the stability of vulnerable atherosclerotic plaques by modulating autophagy, Front. Pharmacol. 9 (2018) 438. https://doi.org/10.3389/fphar.2018.00438.

[16] G. Wang, X. Li, J. Zhao, et al., *Lactobacillus casei* CCFM419 attenuates type 2 diabetes via a gut microbiota dependent mechanism, Food Funct. 8 (2017) 3155-3164. https://doi.org/10.1039/c7fo00593h.

[17] X. Li, E. Wang, B. Yin, et al., Effects of *Lactobacillus casei* CCFM419 on insulin resistance and gut microbiota in type 2 diabetic mice, Benef. Microbes. 8 (2017) 421-432. https://doi.org/10.3920/BM2016.0167.

[18] Y. Zhang, H. Miao, H.Yan, et al., Hepatoprotective effect of *Forsythiae Fructus* water extract against carbon tetrachloride-induced liver fibrosis in mice, J. Ethnopharmacol. 218 (2018) 27-34. https://doi.org/10.1016/j.jep.2018.02.033.

[19] W. Lin, W. Wang, D. Wang, et al., Quercetin protects against atherosclerosis by inhibiting dendritic cell activation, Mol. Nutr. Food Res. 71 (2017) 186-187. https://doi.org/10.1002/mnfr.201700031.

[20] X. Liang, Y. Lv, Z. Zhang, et al., Study on intestinal survival and cholesterol metabolism of probiotics, LWT-Food Sci. Technol.124 (2020) 109132. https://doi.org/10.1016/j.lwt.2020.109132.

[21] X. Liang, Z. Zhang, X. Zhou, et al., Probiotics improved hyperlipidemia in mice induced by a high cholesterol diet via downregulating FXR, Food Funct. 11 (2020) 9903-9911. https://doi.org/10.1039/d0fo02255a.

[22] Q. Xuan, C. Hu, D. Yu, et al., Development of a high coverage pseudotargeted lipidomics method based on ultra-high performance liquid chromatography-mass spectrometry, Anal. Bioanal. Chem. 90 (2018) 7608-7616. https://doi.org/10.1007/s00216-021-03349-w.

[23] Z. Wang, Q. Zhu, Y. Liu, et al., Genome-wide association study of metabolites in patients with coronary artery disease identified novel metabolite quantitative trait loci, Clin. Transl. Med. 11 (2021) e290. https://doi.org/10.1002/ctm2.290.

[24] X. He, X. Chen, L. Wang, et al., Metformin ameliorates ox-LDL-induced foam cell formation in RAW264.7 cells by promoting ABCG-1 mediated cholesterol efflux, Life Sci. 216 (2019) 67-74. https://doi.org/10.1016/j.lfs.2018.09.024.

[25] D. Baci, A. Bruno, C. Cascini, et al., Acetyl-*L*-carnitine downregulates invasion (CXCR4/CXCL12, MMP-9) and angiogenesis (VEGF, CXCL8) pathways in prostate cancer cells: rationale for prevention and interception strategies, J. Exp. Clin. Cancer Res. 38 (2019) 464. https://doi.org/10.1186/s13046-019-1461-z.

[26] F.Y. Chen, J. Zhou, N. Guo, et al., Curcumin retunes cholesterol transport homeostasis and inflammation response in M1 macrophage to prevent atherosclerosis, Biochem. Biophys. Res. Commun. 467 (2015) 872-878. https://doi.org/10.1016/j.bbrc.2015.10.051.

[27] L. Badimon, G. Vilahur, Thrombosis formation on atherosclerotic lesions and plaque rupture, J. Intern. Med. 276 (2014) 618-632. https://doi.org/10.1111/joim.12296.

[28] M.R. Bennett, S. Sinha, G.K. Owens, Vascular smooth muscle cells in atherosclerosis, Circ. Res. 118 (2016) 692-702. https://doi.org/10.1161/CIRCRESAHA.115.306361.

[29] D. Wolf, K. Ley, Immunity and inflammation in atherosclerosis, Circ. Res. 124 (2019) 315-327. https://doi.org/10.1161/CIRCRESAHA.118.313591.

[30] L. Groh, S.T. Keating, L.A.B. Joosten, et al., Monocyte and macrophage immunometabolism in atherosclerosis, Semin. Immunopathol. 40 (2017) 203-214. https://doi.org/10.1007/s00281-017-0656-7.

[31] C. Cochain, A. Zernecke, Macrophages in vascular inflammation and atherosclerosis, Pflugers Arch. 469 (2017) 1-15. https://doi.org/10.1007/s00424-017-1941-y.

[32] D.M. Rocha, A.P. Caldas, L.L. Oliveira, et al., Saturated fatty acids trigger TLR4-mediated inflammatory response, Atherosclerosis 244 (2016) 211-215. https://doi.org/10.1016/j.atherosclerosis.2015.11.015.

[33] Z. Ye, L. Zhong, S. Zhu, et al., The P-selectin and PSGL-1 axis accelerates atherosclerosis via activation of dendritic cells by the TLR4 signaling pathway, Cell Death Dis. 10 (2019) 507. https://doi.org/10.1038/s41419-019-1736-5.

[34] X. Liang, C. Xiu, M. Liu, et al., Platelet-neutrophil interaction aggravates vascular inflammation and promotes the progression of atherosclerosis by activating the TLR4/NF-κB pathway, J. Cell. Biochem. 120 (2019) 5612-5619. https://doi.org/10.1002/jcb.27844.

[35] Y. Li, Y. Wang, Y. Chen, et al., Corilagin ameliorates atherosclerosis in peripheral artery disease via the toll-like receptor-4 signaling pathway *in vitro* and *in vivo*, Front. Immunol. 11 (2020) 1611. https://doi.org/10.3389/fimmu.2020.01611.

[36] T. Liu, L. Zhang, D. Joo, et al., NF-kappaB signaling in inflammation, Signal. Transduct. Target Ther. 2 (2017) 17023. https://doi.org/10.1038/sigtrans.2017.23.

[37] A. Oeckinghaus, S. Ghosh. The NF-kappaB family of transcription factors and its regulation, Cold Spring Harb. Perspect. Biol. 1 (2009) a000034. https://doi.org/10.1101/cshperspect.a000034.

[38] P. Arun, M.S. Brown, R. Ehsanian, et al., Nuclear NF-kappaB p65 phosphorylation at serine 276 by protein kinase A contributes to the malignant phenotype of head and neck cancer, Clin. Cancer Res. 15 (2009) 5974-5984. https://doi.org/10.1158/1078-0432.CCR-09-1352.

[39] S.C. Li, W.F. Hsu, J.S. Chang, et al., Combination of *Lactobacillus acidophilus* and *Bifidobacterium animalis* subsp. *lactis* shows a stronger anti-inflammatory effect than individual strains in HT-29 cells, Nutrients 11 (2019) 969. https://doi.org/10.3390/nu11050969.

[40] K. Yang, J. Xu, M. Fan, et al., Lactate suppresses macrophage pro-inflammatory response to LPS stimulation by inhibition of YAP and NF-κB activation via GPR81-mediated signaling, Front. Immunol. 11 (2020) 587913. https://doi.org/10.3389/fimmu.2020.587913.

[41] E. Sanchez-Rodriguez, A. Egea-Zorrilla, J. Plaza-Díaz, et al., The gut microbiota and its implication in the development of atherosclerosis and related cardiovascular diseases, Nutrients 12 (2020) 605. https://doi.org/10.3390/nu12030605.

[42] V. Bodaghi-Namileh, M.R. Sepand, A.Omidi, et al., Acetyl-*L*-carnitine attenuates arsenic-induced liver injury by abrogation of mitochondrial dysfunction, inflammation, and apoptosis in rats, Environ. Toxicol. Pharmacol. 58 (2018) 11-20. https://doi.org/10.1016/j.etap.2017.12.005.

[43] C.J. Rebouche, Kinetics, pharmacokinetics, and regulation of *L*-carnitine and acetyl-*L*-carnitine metabolism, Ann. N. Y. Acad. Sci. 1033 (2004) 30-41. https://doi.org/10.1196/annals.1320.003.

[44] M.Z. Israr, D. Bernieh, A. Salzano, et al., Association of gut-related metabolites with outcome in acute heart failure, Am. Heart J. 234 (2021) 71-80. https://doi.org/10.1016/j.ahj.2021.01.006.

[45] N. Jamali-Raeufy, F. Alizadeh, Z. Mehrabi, et al., Acetyl-*L*-carnitine confers neuroprotection against lipopolysaccharide (LPS)-induced neuroinflammation by targeting TLR4/NF-κB, autophagy, inflammation and oxidative stress, Metab. Brain Dis. 36 (2021) 1391-1401. https://doi.org/10.1007/s11011-021-00715-6.

[46] S. Wang, J. Xu, J. Zheng, et al., Anti-inflammatory and antioxidant effects of acetyl-*L*-carnitine on atherosclerotic rats, Med. Sci. Monit. 26 (2020) e920250. https://doi.org/10.12659/MSM.920250.

[47] Y. Zheng, P. Lv, J. Huang, et al., GYY4137 exhibits anti-atherosclerosis effect in apolipoprotein $E^{-/-}$ mice via PI3K/Akt and TLR4 signalling, Clin. Exp. Pharmacol. Physiol. 47 (2020) 1231-1239. https://doi.org/10.1111/1440-1681.13298.

[48] G.C. Ferreira, M.C. McKenna, *L*-carnitine and acetyl-*L*-carnitine roles and neuroprotection in developing brain, Neurochem. Res. 42 (2017) 1661-1675. https://doi.org/10.1007/s11064-017-2288-7.